Selective Alteration of the Rate-Limiting Step in Cytosolic Aldehyde Dehydrogenase through Random Mutagenesis[†,‡]

Kwok Ki Ho,[§] Thomas D. Hurley,[||] and Henry Weiner*[,§]

Department of Biochemistry, Purdue University, West Lafayette, Indiana 47907-1153, and Department of Biochemistry and Molecular Biology, Indiana University School of Medicine, Indianapolis, Indiana 46202-5122

Received April 13, 2006; Revised Manuscript Received June 15, 2006

ABSTRACT: Random mutagenesis followed by a filter-based screening assay has been used to identify a mutant of human class 1 aldehyde dehydrogenase (ALDH1) that was no longer inhibited by Mg^{2+} ions but was activated in their presence. Several mutants possessed double, triple, and quadruple amino acid substitutions with a total of seven different residues being altered, but each had a common T244S change. This point mutation proved to be responsible for the Mg^{2+} ion activation. An ALDH1 T244S mutant was recombinantly expressed and was used for mechanistic studies. Mg^{2+} ions have been shown to increase the rate of deacylation. Consistent with the rate-limiting step for ALDH1 being changed from coenzyme dissociation to deacylation was finding that chloroacetaldehyde was oxidized more rapidly than acetaldehyde. Furthermore, Mg^{2+} ions only in the presence of NAD(H) increased the rate of hydrolysis of *p*-nitrophenyl acetate showing that the metal only affects the binary complex. Though the rate-limiting step for the T244S mutant was different from that of the native enzyme, the catalytic efficiency of the mutant was just 20% that of the native enzyme. The basis for the change in the rate-limiting step appears to be related to NAD^+ binding. Using the structure of a sheep class 1 ALDH, it was possible to deduce that the interaction between the side chain of T244 and its neighboring residues with the nicotinamide ring of NAD^+ were an essential determinant in the catalytic action of ALDH1.

Human cytosolic, class 1 and mitochondrial, class 2 aldehyde dehydrogenases (ALDH1[1] and ALDH2) are members of a superfamily of enzymes that catalyze the irreversible oxidation of a variety of aldehydes to their corresponding carboxylic acids in an $NAD(P)^+$-dependent reaction (*1*). The level of overall amino acid identity between the two isozymes is high (∼70%) (*2*). A comparison of the available crystal structures suggests that both isozymes are very similar in overall tertiary structure, coenzyme binding, and active sites (*3*, *4*). Both isozymes share the same catalytic mechanism for aldehyde oxidation (Figure 1). Despite the overall similarities in their reactions, ALDH1 and ALDH2 differ in the step that is rate limiting and can be differentiated by the way in which their maximal catalytic rates are affected by Mg^{2+} ions. The rate-limiting step is coenzyme dissociation for ALDH1 (*6*) and deacylation for ALDH2 (*7*, *8*). For both isozymes, Mg^{2+} ions appear to enhance the rate of deacylation, inhibit the rate of coenzyme dissociation, and have no effect on the formation of a covalent adduct with the enzyme or hydride transfer (*5*). Thus, when assayed under V_{max} conditions, Mg^{2+} ions appear to inhibit the activity of ALDH1 and activate ALDH2, as would be predicted for isozymes with their respective rate-limiting steps (*5*).

During the catalytic cycle, the nicotinamide ring of NAD^+ moves between two discrete locations (*3*, *4*). X-ray crystallographic studies of ALDH 1 and ALDH2 have identified two conformations: one with an extended nicotinamide ring that favors hydride transfer and the other with a contracted ring that favors the action of the general base for deacylation (*3*, *9*−*11*). The occurrence of different conformations at the nicotinamide ring has also been found in NMR and fluorescence studies of ALDH1 and ALDH2 (*12*). It is necessary for the nicotinamide ring to change conformations during the catalytic cycle in order to allow the appropriate active site components to participate in distinct chemical processes during the catalytic cycle. If this movement did not occur, then one or more of the reactions would not be able to proceed. The flexible interactions that occur between the coenzyme and complementary groups on the enzyme appear to facilitate these changes in coenzyme conformation (*3*, *4*). In the case of ALDH2 but not ALDH1, Mg^{2+} ions appear to induce a bias toward a particular conformation of the nicotinamide ring, which might indicate subtle differences in the interaction of the respective enzymes with the coenzyme (*12*). Understanding such differences could help identify the structural determinants necessary to confer to a specific step the capacity of being rate limiting. The majority of the amino acid residues interacting with the coenzyme are conserved between ALDH1 and ALDH2 (*1*). In ALDH2, structural data have pointed out the importance of some of these residues (*9*), and site-directed mutagenesis has dem-

[†] This research was supported by NIH Grant AA05812.

[‡] This is article no. 2006-17969 from Purdue University Agriculture Experiment Station.

* To whom correspondence should be addressed. Tel: (765) 494-1650. Fax: (765) 494-7897. E-mail: hweiner@purdue.edu.

[§] Purdue University.

[||] Indiana University School of Medicine.

[1] Abbreviations: ALDH, aldehyde dehydrogenase; ALDH1, human liver cytosolic aldehyde dehydrogenase; ALDH2, human liver mitochondrial aldehyde dehydrogenase.

10.1021/bi060718c CCC: $33.50
Published on Web 07/18/2006

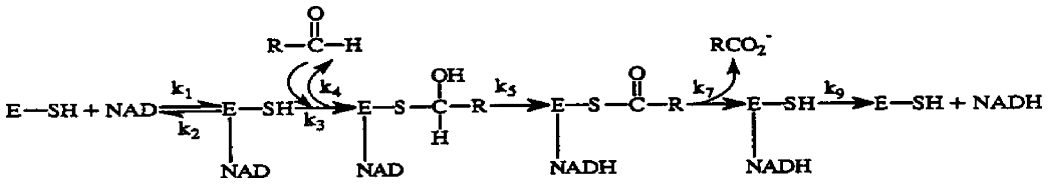

FIGURE 1: Reaction scheme for the dehydrogenase activity catalyzed by ALDH.

onstrated the crucial role of a few in catalysis (*13*−*15*). Similarly, the structure of sheep liver class 1 ALDH confirms the presence of similarly interacting residues (*4*). Although a crystal structure for the human ALDH1 is not available, the enzymes share 92% sequence identity and would not be predicted to vary considerably in structure. Consequently, an investigation of the effect of altering amino acid residues related to enzyme chemistry in the human enzyme should afford data to elucidate their role in catalysis relative to that in the structural model derived from sheep ALDH1 structure. Furthermore, such data can be used to validate a homology model of human ALDH1. Here, we have developed a method based on random mutagenesis and filter-based screening to identify mutations that reverse the inhibitory response of ALDH1 to Mg^{2+} ions. We rationalized that such mutations are likely to affect the enzymatic steps of deacylation and NADH dissociation. Random mutagenesis was employed here because Mg^{2+} ions have so far only been identified to interact directly with the coenzyme. Data obtained from screening and other studies, including site-directed mutagenesis, steady-state kinetics, and computer modeling, show that T244 is an essential determinant in the enzymatic mechanism of ALDH1 and may directly impact the rate of deacylation.

EXPERIMENTAL PROCEDURES

Chemicals. All chemicals used for enzyme assays and purifications were purchased from Sigma (St. Louis, MO) or Aldrich (Milwaukee, WI). B-PER reagent was purchased from Pierce (Rockford, IL). HPLC purified oligonucleotide primers were synthesized by IDT (Coralville, IA). T_4 DNA ligase, the restriction enzymes *BamH*I and *Nde*I and ITPG were obtained from New England Biolabs (Beverly, MA). DNA purification kits were purchased from Qiagen (Valenica, CA). Random and site-directed mutagenesis kits were obtained from Stratagene (La Jolla, CA). Unless otherwise stated, all chemicals were used without further purification.

Bacterial Strains and Plasmids. All random and site-directed PCR mutagenesis experiments were performed on a full-length ALDH1 cDNA cloned in a pT7-7 plasmid (*16*). *Escherichia coli* BL21(DE3)pLysS and DH5α cell strains were obtained from Stratagene and Gibco BRL (Life Technologies, Grand Island, NY) and stored as frozen glycerol stocks.

Library Construction and Screening. Random mutagenesis of the ALDH1 gene was conducted by using error-prone PCR. Mutations were introduced under low-frequency conditions according to the Stratagene GeneMorph PCR Mutagenesis kit. Two oligonucleotides flanked by the *BamH*I and *Nde*I restriction sites, 5′CAGGTCGACTCT AGAGGATC-CTTA-3′ and 5′-CCACAACGGTTTCCCTCTAGA-3′, were used as forward and reverse primers, respectively. The PCR products were gel purified by using a Qiagen QIAquick Spin kit, and some were used as templates in a second error-prone PCR reaction. The gel purified PCR products from the first and second reactions were pooled and ligated with *BamH*I and *Nde*I digested pT7-7. BL21(DE3)pLysS competent cells were transformed with the ligated DNA and plated onto Luria−Bertani (LB)/ampicillin (75 μg/mL) agar plates. The transformants were inoculated into 1.5 mL of Eppendorf microcentrifuge tubes containing 0.5 mL of LB/ampicillin. The cells were grown for about 60 min at 37 °C with shaking at 250 rpm and kept as stocks. The cells from individual stocks (1 μL each) were spotted onto supported nitrocellulose filters (Schleicher & Schuell, Keene, NH) that laid onto LB/ampicillin agar plates supplemented with 100 μg/mL of ITPG. A grid was marked off on the bottom of the plates to guide the spotting of cells at the appropriate positions. The sample filters were prepared in duplicate and kept for about 2 h at 37 °C. After another 2 h at 4 °C, the filters were laid colony side up on a series of filter papers that had been soaked with the following solutions: (i) 25 mM sodium phosphate buffer (pH 8.0) containing 1 mg/mL of lysozyme and 1 mM EDTA for 30 min; (ii) 10 mM sodium phosphate buffer (pH 8.0) containing 0.1% B-PER reagent and 1 mM EDTA for 30 min; and (iii) 10 mM sodium phosphate buffer (pH 8.0) containing 1mM EDTA for 30 min. Then the filters were placed in Petri dishes containing 10 mM sodium phosphate buffer (pH 7.5) and washed for 15 min on a rocker platform that sent small waves of the phosphate buffer over their surfaces. The washed filters were air-dried and placed in a reaction buffer containing 25 mM sodium phosphate (pH 7.5), 1.5 mM NAD^+, 3.5 mM pyrazole, 6 mM sodium pyruvate, 1 mM nitroblue tetrazolium, and 13 μM phenazine methosulfate for the staining of ALDH1 activity. The reaction was started by adding 100 μM propionaldehyde. In the presence of phenazine methosulfate, NADH reduced nitroblue tetrazolium to an insoluble blue-purple complex. After 15 to 30 min, the wet filters were laid on dry filter papers, allowing the color to develop. For comparative purpose, one set of the duplicate filters was stained in the presence of 300 μM $MgCl_2$. Clones showing increased activity in the presence of Mg^{2+} ions were screened again as before by using cells from the original stocks and a substrate concentration diluted 2-fold. Crude cell extracts from the resulting positives were further analyzed fluorometrically for the presence of Mg^{2+}-ion increased dehydrogenase activity. To prepare the crude cell extracts, the cells from the original stocks were inoculated into 100 mL of LB/ampicillin and were grown at 37 °C with rigorous shaking until the OD_{600} value reached 0.5−0.6. The cells were then induced for 12 h by 2 mM ITPG at 18 °C with gentle shaking at 50 rpm. The cells were harvested by centrifugation at 3000*g* for 10 min at 4 °C and washed once in 0.9% sodium chloride solution. After resuspending in 10 mM sodium phosphate buffer (pH 7.5) that contained 1 mM EDTA and 1 mM dithiothreitol, the cells were disrupted by a French Press cell (3 cycles at 15 000 psi) pre-chilled on ice. The insoluble materials were removed by centrifugation at

30 000*g* for 30 min at 4 °C. The supernatants were filtered through a 0.8/0.2 μm Acrodisc Supor membrane (Gelman laboratory, Ann Arbor, MI) and used as clarified cell lysates.

Site-Directed Mutagenesis and Cloning of the T244S Mutant. The T244S mutation of the ALDH1 gene was introduced by using the Stratagene Quick Change II Site-Directed Mutagenesis kit and a pair of complementary oligonucleotide primers, 5′GACAAAGT AGCCTTCTCAG-GATCAACAGAGGTTGG-3′ and 5′-CCAACCTCTGT-TGATCCTGAGAAGGCTACTTTGTC-5′. The base changes that are required to change the desired codon are underlined. The resulting plasmids were amplified in DH5α competent cells and screened for the desired mutation by DNA sequencing. The T244S plasmid was subcloned into BL21-(DE3)pLysS and was used for protein expression.

Expression and Purification of ALDH1 and the T244S Mutant. All enzymes were expressed and purified as described previously (*17*, *18*). Briefly, the recombinant enzymes were purified by protamine sulfate treatment (1.25 mg/mL) followed by DEAE-cellulose column and *p*-hydroxyacetophenone (HAP) affinity chromatography. The purified enzymes were homogeneous as indicated by SDS−PAGE (*19*). The fractions containing individual purified enzymes were pooled and concentrated by Centricon centrifugal filters (Millipore, Bedford, MA). Prior to subsequent characterization, the concentrated enzymes were stored in 50% glycerol at −20 °C and appeared to be stable for at least six months.

Fluorescence and Absorbance Assay for Dehydrogenase Activity. The dehydrogenase activity assays were performed by measuring the rate of increase in the fluorescence or absorbance of NADH formation in 50 mM sodium phosphate or 25 mM Hepes (pH 7.4) at 25 °C. The K_m and V_m values for NAD^+ were determined in the presence of 140 μM propionaldehyde. The K_m and V_m values for propionaldehyde were determined in the presence of 1 mM NAD^+. The dissociation constants for NAD^+ (K_{ia}) were determined by bisubstrate kinetic analysis (*20*). The dissociation constants of NADH (K_{iq}) were determined as inhibition constants using NADH as a competitive inhibitor against NAD^+. The K_{iq} for NADH was determined with a constant saturating concentration of 140 μM propionaldehyde and a varied concentration of NAD^+. Linear regression analysis of a double-reciprocal plot or a Dixon plot was used for calculating the value of K_{iq} (*21*). The buffer and Mg^{2+} ion concentrations used are indicated for each experiment.

Spectrophotometric Assay for Esterase Activity. The esterase activities of the recombinant enzymes were determined at 400 nm by measuring the rate of *p*-nitrophenol formation in 50 mM Pipes (pH 7.4) with 0−500 μM *p*-nitrophenyl acetate. For the effect of NAD(H) alone or together with Mg^{2+} ions on the enzymes, assays were conducted using 150 μM *p*-nitrophenyl acetate and a coenzyme concentration ranging from 5 to 200 μM. The Mg^{2+} ion effect on the esterase reaction was measured in the presence of 250 μM $MgCl_2$. A molar extinction coefficient of 18.3×10^3 ($M^{-1}cm^{-1}$) at 400 nm for *p*-nitrophenolate was used for calculating its rate of formation.

Kinetic Measurements. All measurements for dehydrogenase and esterase activities were performed in triplicate and averaged. The standard errors were within ±15%.

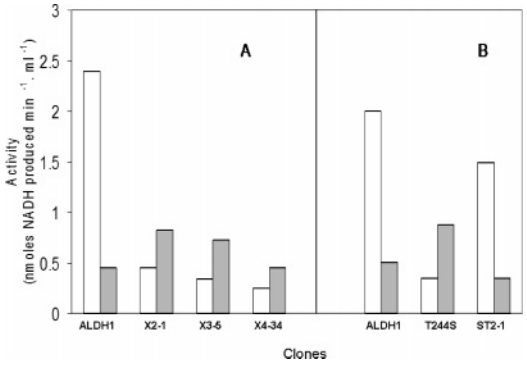

FIGURE 2: Dehydrogenase activities of clarified cell lysates prepared from clones selected during screening of ALDH1 mutants. Lysate samples were assayed according to Experimental Procedures in the presence (gray bars) and absence (clear bars) of 200 μM $MgCl_2$ and compared with ALDH1 (1) in both panels. (A) Randomly mutated clones, X2-1 (2), X3-5 (3), and X4-34 (4). (B) Site-directed mutagenesis was used for reverting Ser244 in X2-1, X3-5 and X4-34 back to a threonine. A single mutant, T244S, was created using the coding sequence of ALDH1, and the other revertants, ST2-1, ST3-5, and ST4-34, were obtained from X 2-1, X3-5, and X4-34, respectively. The results obtained for ST3-5 and ST4-34 were similar to that for ST2-1 and were not included in the Figure. The activities of individual mutants were measured in two independent cultures and normalized to the OD_{600} of each culture. The values shown represent the average of the two measurements.

Determination of Protein Concentration. A protein assay kit (Bio-Rad Laboratories, Hercules, CA) with bovine serum albumin as a standard was used for determining protein concentration.

RESULTS

Isolation of ALDH1 Mutants with Mg^2-Ion Increased Activity. The rate-limiting step for ALDH1 has been shown to be the dissociation of NADH from the enzyme, and it has also been shown that Mg^{2+} ions further slow this step (*5*). To determine whether this step could be altered, random mutations were introduced into the ALDH1 gene using the method of error-prone PCR. A library of ≈4000 ALDH1 mutants was expressed in *Escherichia coli*, immobilized on nitrocellulose membranes and lysed for the rapid screening of dehydrogenase activity. The reaction was based on the formation of a purple formazan as a result of coupling the NAD^+-dependent oxidation of propionaldehdye to the reduction of nitroblue tetrazolium in the presence of phenazine methosulfate. Fifty potential ALDH1 mutants were identified that exhibited higher activity in the presence of Mg^{2+} ions. Five of these ALDH1 mutants were confirmed to possess Mg^{2+}-dependent increases in activity after a second screening at a lower substrate concentration. Verification of the Mg^{2+}-ion effect was conducted by using clarified cell lysates of cells expressing these ALDH1 mutants (Figure 2A).

DNA sequencing revealed that clones X2-1 and X2-14 had two identical mutations, T244S/D391E, X3-5 and X3-7 had three identical mutations, S33C/T244S/C463S, and X4-34 had four mutations, S31T/V63A/T244S/E479D. Because all these ALDH1 mutants have the same T244S mutation, site-directed mutagenesis was used for reverting Ser244 back to a threonine in X2-1, X3-5, and X4-34 to study its effect on the Mg^{2+}-ion effect on the dehydrogenase activity. X2-14 and X3-7 were not investigated further because their mutations were identical to those of X2-1 and X3-5,

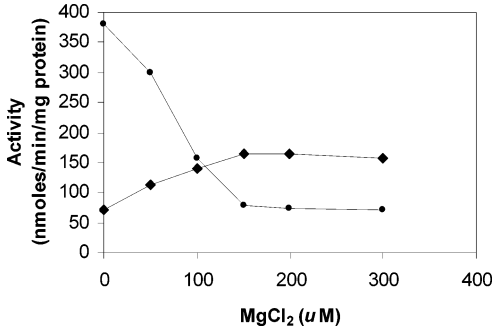

FIGURE 3: Effect of Mg^{2+} ions on the dehydrogenase activity of ALDH1 (●) and the T244S mutant (♦). Assays were conducted in a phosphate buffer (pH 7.4) in 1 mM NAD^+ and 140 μM propionaldehyde as described in Experimental Procedures.

respectively. As shown in Figure 2B, clarified cell lysates prepared for the respective revertants designated ST2-1, ST3-5, and ST4-34 were found devoid of Mg^{2+}-ion increased activity. Instead, their enzyme activities were inhibited by Mg^{2+} ions just as ALDH1 was. An ALDH1 mutant with a single mutation, T244S, was created by using site-directed mutagenesis. The clarified cell lysate of this ALDH1 mutant showed Mg^{2+}-ion increased activity, confirming that the single mutation alone was responsible for the Mg^{2+}-ion effect.

Effect of Mg^{2+} Ions on the Dehydrogenase Activity of ALDH1 and Its T244S Mutant. Figure 3 shows the effect of increasing concentrations of Mg^{2+} ions on their dehydrogenase activities. Although ALDH1 activity decreased with increasing concentration of Mg^{2+} ions, the T244S mutant activity increased. ALDH1 lost about 70% of its activity in the presence of 200−250 μM but still retained about 15−20% of its activity when the Mg^{2+} ions were increased to 400−500 μM. Such an inhibitory pattern would be expected for a cytosolic, class 1 ALDH, whose rate-limiting step was NADH dissociation (*6*). In the absence of Mg^{2+} ions, the T244S mutant had less than 20% of the specific activity of ALDH1. However, its activity increased 100% at 200−250 μM Mg^{2+} ions and remained relatively unchanged at further increases of Mg^{2+} ions, up to 400 μM. This Mg^{2+}-ion activating effect bore a resemblance to the metal ion effect observed with ALDH2, whose rate-limiting step was deacylation (*7*, *8*). The Mg^{2+}-ion activation was further investigated by using varied concentrations of the metal ion and NAD^+ at a saturating concentration of propionaldehyde. The data were converted to double reciprocal plots, giving rise to a series of intersecting lines at a common point above the abscissa of the second quadrant (data not shown). This result showed that the V_m increased with increasing Mg^{2+} ion concentrations, while the K_m for NAD^+ decreased. Even though the K_m value for NAD in a two substrate reaction is not strictly related to binding, the observation suggests that coenzyme binding might have a role in the activating effect of Mg^{2+} ions on the T244S mutant.

Steady-State Kinetics of ALDH1 and the T244S Mutant. Bisubstrate kinetics were performed for both enzymes by using varied concentrations of NAD^+ and propionaldehyde to determine if K_{ia} indeed was affected by Mg^{2+} ions. The kinetic data obtained for either enzyme were compatible with a sequential kinetic mechanism consistent with what has been shown to occur with class 1 and class 2 ALDH. Table 1 summarizes the kinetic constants of ALDH1 and the T244S mutant and the effect of Mg^{2+} ions on their kinetic constants. In ALDH1, the kinetic constants were consistent with those obtained previously (*5*, *22*). The T244S mutant had a smaller k_{cat} value that was less than 20% of the value for ALDH1. This marked decrease in the k_{cat} value was accompanied by a 5- and 9-fold increase in Michaelis (K_a) and dissociation constant (K_{ia}) values, respectively, of the T244S mutant for NAD^+. In contrast, the Michaelis (K_b) constant for propionaldehyde and the dissociation constant (K_{iq}) values for NADH were similar in both enzymes. Thus, the T244S mutation appears to have an effect on both k_{cat} and coenzyme binding. Catalytic efficiency as calculated by k_{cat}/K_{ia} K_b (*23*) decreased by more than 80-fold in the T244S mutant compared with that of ALDH1. The presence of Mg^{2+} ions increased the k_{cat} value of the T244S mutant by 100%. The k_{cat} value of the T244S mutant in the presence of Mg^{2+} was higher than ALDH1 under similar conditions but was still less than 40% of ALDH1 in the absence of Mg^{2+} ions. The presence of Mg^{2+} ions produced a small decrease in K_{ia}, K_a, and K_{iq}, and the fold decrease in each was similar between the two enzymes, suggesting that Mg^{2+} ions tightened the binding of NAD^+ and NADH with the T244S mutant as had been observed with ALDH1 (*5*). It also decreased the K_b of ALDH1 by about 2-fold but seemed not to affect that of the T244S mutant. The catalytic efficiency was actually improved slightly in ALDH1 despite having a decreased k_{cat} value, and it was largely due to a decrease in the K_{ia}value. In contrast, the increase in the k_{cat} value combined with the decrease in the K_{ia} value gave rise to a 14-fold increase in the catalytic efficiency of the T244S mutant. The finding that Mg^{2+} ions had the same effect on coenzyme binding in either enzyme but an opposite effect on their k_{cat} values suggested the rate-limiting step in the T244S mutant was no longer NADH dissociation. This observation was further investigated by using chloroacetaldehyde because the electron-withdrawing effect of the chloro group will increase the hydolysis of the acyl intermediate. It is known that chloroacetaldehyde is oxidized 2−3 times faster than acetaldehyde by ALDH2 under V_{max} conditions, consistent with an enzyme whose rate-limiting step was deacylation (*15*). As shown in Table 2, chloroacetaldehyde was oxidized just as fast as acetaldehyde by ALDH1. In contrast, chloroacetaldehyde was

Table 1: Effect of Mg^{2+} Ions on the Kinetic Constants[a] of ALDH1 and the T244S Mutant

	ALDH1		T244S mutant	
	without Mg^{2+}	with Mg^{2+}	without Mg^{2+}	with Mg^{2+}
kinetic constant				
K_{cat} (min^{-1})	89	25	16	33
K_m (NAD^+) (μM)	14.5	3.6	75.5	28
K_m (propionaldehyde) (μM)	5.8	3.4	9.6	8.7
K_{ia} (μM)	6.5	1.5	58	9.5
K_{iq} NADH (μM)[b]	45	25	55	20

[a] Assays were conducted as described in Experimental Procedures, using a 50 mM sodium phosphate buffer (pH 7.4) in the presence of 0 or 250 μM $MgCl_2$. [b] The K_{iq} value for NADH was determined in separate experiments as an inhibition constant (*21*). Assays for K_{iq} were conducted in 25 mM Hepes (pH 7.4), using 0 or 250 μM $MgCl_2$ as described in Experimental Procedures.

Table 2: Acetaldehyde and Chloroacetaldehyde as Substrates for ALDH1 and the T244S Mutant in the Presence and Absence of Mg^{2+} Ions

	$V_{chloroacetaldehyde}/V_{acetaldehyde}$[a]	
enzyme	$-MgCl_2$	$+ MgCl_2$
ALDH1	1.2	1.0
T244S mutant	3.4	2.2

[a] The reaction velocity for individual substrates was determined at V_{max} conditions using 50 mM phosphate buffer (pH7.4) with 1.5 mM NAD^+ and substrate concentrations ranging from 5 to 250 μM in the presence and absence of 250 μM $MgCl_2$.

Table 3: Relative Maximal Activities for the Esterase Reaction of ALDH1 and the T244S Mutant in the Presence and Absence of Coenzymes and Mg^{2+} Ions[a]

	ALDH1	T244S mutant
conditions		
$+Mg^{2+}$	1	1
$+NAD^+$	4.8	2
$+NAD^+/Mg2^+$	4.6	4
+NADH	2.5	5
$+NADH/Mg2^+$	6.6	10

[a] The values for relative maximal velocities were obtained by comparing the values of maximal velocities obtained from reciprocal plots ($1/v - v_o$ vs 1/coenzyme). The values v_o and v were taken in the absence of both the coenzyme and Mg^{2+} ions and in the presence of either the coenzyme alone or together with 250 μM $MgCl_2$, respectively. The metal ion alone had no activating effect on either ALDH1 or the T244S mutant. The maximal velocities determined in the presence of the metal ion were 36 and 8 nmol/mg/min for ALDH1 and the T244S mutant, respectively, and set equal to 1 as the standard. Assays were conducted in 50 mM Pipes buffer (pH7.4) as described in Experimental Procedures.

oxidized 2−3 times faster than acetaldehyde with the T244S mutant in the presence and absence of Mg^{2+} ions, consistent with possessing a rate-limiting step similar to that of ALDH2.

Effect of Mg^{2+} Ions on the Esterase Activity of ALDH1 and the T244S Mutant. From the results presented earlier, it is clear that the dehydrogenase reaction was greatly affected by the T244S mutation. ALDH1 can also catalyze an esterase reaction, the mechanism of which is similar to that of the dehydrogenase reaction except that it does not have a hydride transfer step (*8*, *24*, *25*). It was previously shown that the rate-limiting step for the esterase reaction for *p*-nitrophenyl acetate was acyl-enzyme hydrolysis with the sheep isozyme (*26*). To look at how this step may be affected by the T244S mutation, the esterase activity of ALDH1 and the T244S mutant were measured in the presence and absence of Mg^{2+} ions. *p*-Nitrophenyl acetate was used up to 500 μM. Further increase in the substrate concentration resulted in nonlinear Lineweaver−Burk plots, as reported earlier (*22*). The esterase activity of the T244S mutant was markedly reduced compared with that of ALDH1. Table 3 summarizes the effects of NAD(H) alone or together with Mg^{2+} ions on their esterase reaction. Like ALDH1, the esterase activity of the T244S mutant remained relatively unchanged in the presence of Mg^{2+} ions but displayed an increase in activity in the presence of NAD^+ and NADH. The NADH-activated activity of either enzyme was enhanced by Mg^{2+} ions. In contrast, the metal ion produced a small increase (2-fold) in the NAD^+-activated activity of the T244S mutant but no significant change in that of the native enzyme.

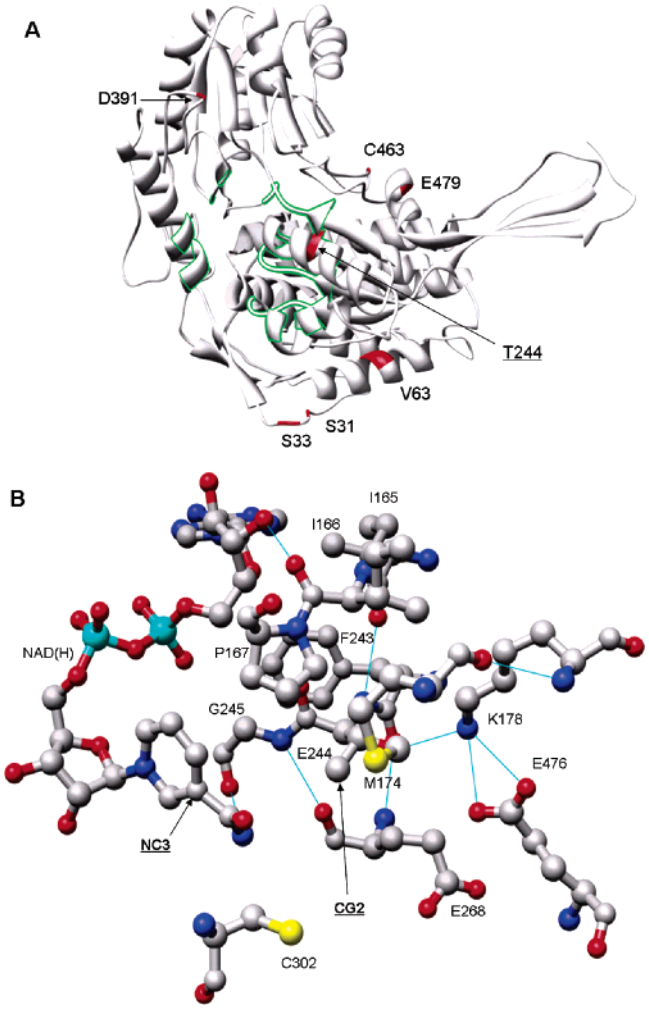

FIGURE 4: (A) Schematic drawing of the model structure for ALDH1. The various randomly mutated residues are colored red. The putative NAD^+ binding site identified by superposing the sheep cytosolic ALDH (pdb 1BXS) onto ALDH1 is colored green. (B) Schematic drawing of the structural model for ALDH1 showing NAD^+ and the other amino acid residues that lie within a radius of less than 4 Å with respect to T244. Putative hydrogen bonds were colored blue. The contracted conformation of NAD^+ in the sheep enzyme structure was superposed onto the model structure for ALDH1. As a point of reference, C302 on the re-side of the nicotinamide ring was included in the diagram. Superposing structures were obtained by using the UCSF Chimera program (http://www.cgl.ucsf.edu/chimera/).

Computer Modeling of ALDH1. In the absence of crystallographic data for human ALDH1, a comparative model for ALDH1 was built on the basis of the solved crystal structure of the sheep isozyme (pdb structure, 1BXS). The model structure for ALDH1, residue 7−500, was generated using the program Swiss-Pdb Viewer and the Swiss-Model server (http://www.expasy.org/spdbv/) (*27*−*29*). The root-mean-square displacement between the backbone α-carbons of the sheep structure and the ALDH1 model structure was less than 0.1 Å, and no further energy minimization procedures were performed with the model structure. As expected from the high sequence identity (92%), the overall tertiary structure for ALDH1 and the amino acid residues involved in coenzyme binding and catalysis are highly conserved between the two proteins. Figure 4A shows the model structure for ALDH1 and the locations of the randomly mutated residues. Of the different residues, only T244 appeared to

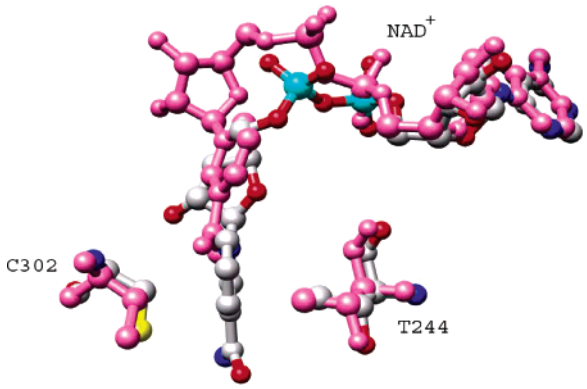

FIGURE 5: Comparison of the coenzyme binding site in ALDH1 and ALDH2. The structural models of the ALDH1 and ALDH2−NADH binary complex (pdb structure, 1CW3) were overlaid on the basis of the orientations of the ALDH1 monomer (colored pink) and chain B of ALDH2 (colored element) using the DeepView/Swiss-PDB Viewer program (http://us.expasy.org/spdbv/). Both conformations for NAD^+ in ALDH2 are illustrated here to show that the nicotinamide ring moves close to within 3 Å from T244 following coenzyme isomerization.

be located close to the catalytic and coenzyme binding sites. Figure 4B shows the amino acids that lie within 4 Å of T244 of the ALDH1 structure and the contracted NAD^+ structure of the sheep enzyme superposed onto the ALDH1 structure. These amino acids and their spatial positions are conserved in the sheep enzyme structure, and the contracted nicotinamide ring appears too far from interacting with T244 directly. It should be noted that there is considerable flexibility in the conformation of the E268 side chain in the template structure of the sheep isozyme, a reflection of the weak electron density and high B factors obtained for the residue (*3*). Such flexibility is thought to be inherent to the residue, and multiple conformations are observed in structures of many ALDH family members. Thus, the position of the side chain shown here represents only one of the possible conformations, and other conformations do not interfere with the binding of an extended nicotinamide conformation required for hydride transfer (*3*, *4*, *11*). In the model structure, the contracted nicotinamide ring is not close enough to make direct contact with T244 (Figure 4). The closest approach of the CG2 atom of T244 and the NC3 of NAD^+ is more than 5 Å. A hydrophobic interaction between an extended nicotinamide ring and the CG2 atom of T244 is observed in the crystal structures of ALDH2 (pdb structures, 1O00 and 1CW3). To find out whether an extended conformation of NAD^+ could interact directly with T244, we compared the coenzyme binding site of ALDH1 and the ALDH2−NAD^+ binary complex after a superimposition of the enzymes on the basis of their Cα atoms (Figure 5). The superimposition revealed that that the active and coenzyme binding sites are similar both in the nature of amino acids and their spatial relationships. A similarly positioned nicotinamide ring in ALDH1 would position the CG2 atom of T244 within 2.7Å of the NC4 atom of NADH, close enough to form van der Waals contacts with the nicotinamide ring.

DISCUSSION

The rate-limiting step for an enzyme reaction can often be determined from a combination of various kinetic studies. What is unique among aldehyde dehydrogenases is that for the three major classes of enzyme that have been investigated, the rate-limiting step is different for each (*13*, *22*, *30*−*36*). The effect of Mg^{2+} ions on the specific activity of the isozyme has been a useful tool to elucidate the rate-limiting step for the different forms. Here, we have shown that the mutation of a single amino acid, T244S, can produce an ALDH1 mutant with an altered response to the presence of Mg^{2+} ions. Though other mutant forms of the enzyme were produced, it appears that the point mutation at position 244 was solely responsible for the change in properties in the mutants compared to that of the native enzyme. Instead of being inhibited by the metal ion as was observed with ALDH1, the T244S mutant was activated. ALDH2 displays a similar Mg^{2+}-dependent activation. This effect is found when the rate-limiting step as depicted in the postulated enzyme mechanism is the deacylation step (Figure 1). Essentially, the overall reaction involves the binding of an aldehyde to an initial binary complex of NAD^+ with ALDH to form a thiohemiacetal intermediate, which is then oxidized to a thioacyl intermediate. Mg^{2+} ions are thought to promote deacylation of the thioacyl intermediate, a step before NADH dissociation. This could be due to an increased activation of the general base involved in the deacylation or be achieved by promoting a conformational change of the coenzyme to one that favors deacylation (*11*). Magnesium ions appear to bind to the actual NAD(H) moiety and only indirectly to the enzyme. Thus, the effect of the ion is only observed when NAD(H) is present. That the esterase reaction rate was altered by Mg^{2+} ions only in the presence of NAD(H) supports this latter observation (Table 3).

The T244S mutant and ALDH2 may now have the same rate-limiting step, as suggested by their similar response to Mg^{2+} ions and their shared ability to oxidize chloroacetaldehdye faster than acetaldehyde. Actually, the ratio between the T244S mutant activities with chloroacetaldehyde and acetaldehyde was between 3 and 4 (Table 2). Such a ratio has previously been reported for ALDH2 (*15*). It was also found that the T244S mutant activity toward chloroacetaldehyde was not further enhanced by the presence of Mg^{2+} ions. Chloroacetaldehyde is still a better substrate for the T244S mutant than acetaldehyde in the presence of Mg^{2+} ions, but it appears that the chloro-acyl intermediate might be hydrolyzed at a rate that could not be increased further by Mg^{2+} ion activation of the general base or through metal ion acceleration of any coenzyme conformational change.

The esterase activity was originally thought to be of nonphysiological importance. Recently, though, it has been shown that ALDH hydrolyzes nitroglycerine, and this step is necessary for vasodilatation to occur in patients taking the drug (*37*−*40*). Both the dehydrogenase and esterase reactions share the common deacylation step (*40*). Decrease in the nitrophenyl esterase activity of the T244S mutant provided further evidence that the T244S mutation affected the deacylation reaction.

The k_{cat} value for the oxidation of propionaldehyde by the T244S mutant in the absence of Mg^{2+} ions was just 20% of that of ALDH1. Mg^{2+} ions slow the rate-limiting dissociation of NADH from the ALDH1−NADH binary complex (*5*). This finding was reflected by a decreased K_{iq} value for ALDH1 and was reconfirmed here. The K_{iq} value for the T244S mutant, however, was similar to that for ALDH1 (Table 1) showing that Mg^{2+} ions still affected NADH

binding, but because dissociation was no longer rate liming, we did not observe a kinetic effect on the specific activity of the T244S mutant. We examined the dissociation of NADH from both enzymes using a displacement experiment that measured the change in the fluorescence of NADH because the coenzyme was displaced from an enzyme−NADH binary complex by the addition of excess NAD^+. Our fluorescent data (not shown) confirmed that the dissociation of NADH was similar for both ALDH1 and the T244S mutant, indicating that the decreased turnover of the T244S mutant was unrelated to NADH dissociation. Indeed, these observations that the mutation had little effect on NADH binding or release is consistent with the structural observation that T244 does not directly interact with NADH when it is bound in the contracted (hydrolysis) position.

In contrast to the relatively minor changes in NADH binding, the K_m and K_{ia} values for NAD^+ were 5- and 9-fold higher, respectively, in the T244S mutant than in ALDH1. For the T244S mutant, the association rate for NAD^+, k_1, as measured by k_{cat}/K_m (*41*) decreased by 30-fold. It is not unexpected that the binding of NAD^+ was affected by the addition of Mg^{2+} ions. When binding to ALDH1 or ALDH2, the nicotinamide ring of the coenzyme samples different conformations, whereas the adenine portion remains relatively immobile (*12*). Two conformations, one contracted (hydrolysis) and one extended (hydride transfer) have been identified by X-ray crystallographic studies of human ALDH2 and other mammalian class 1 and 2 isozymes (*3*, *9*−*11*). Although the contracted conformation favors the action of the general base for the deacylation step, the extended conformation favors hydride transfer. It is possible that ALDH1 has no preference to bind a particular conformation. Therefore, it can be expected that NAD^+ occupies both conformations with nearly equal residency times because the rate-limiting step is neither deacylation nor hydride transfer but is NADH dissociation. However, for efficient hydride transfer, the oxidized coenzyme must be held near C302 and thereby interact with the side chain of T244. Conceivably, the mutation to T244 could shift the enzyme's preference toward the extended conformation of the coenzyme resulting in both a decrease in coenzyme binding and an increase in the residency time for the extended conformation. The presence of Mg^{2+} ions could not only improve the binding of the coenzyme as indicated by the decreased K_{ia} value but also accelerate the conformational change of the coenzyme in the T244S mutant, as was observed with ALDH2, and thus increase the rate of deacylation. This explanation is consistent with the finding that the esterase activity of the T244S mutant was much lower than that of ALDH1 and that the presence of Mg^{2+} ions had a differential effect on ALDH1 and the T244S mutant with respect to NAD^+ activation (Table 3). Because the deacylation step is common to both esterase and dehydrogenase reactions, it may be no coincidence that both reactions were affected by the T244S mutation and responded in a similar manner to the presence of Mg^{2+} ions.

Alternatively, the increased volume of the active site resulting from the T244S mutation might permit an increased residency time for the reduced form of the coenzyme in the extended conformation such that the isomerization out of the active site is slowed, and Mg^{2+} accelerates this process. This possibility is supported by the structural evidence that

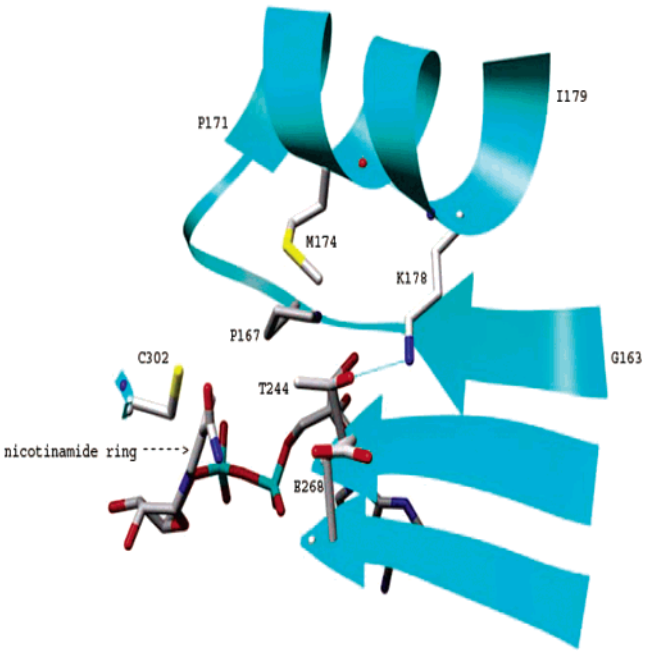

FIGURE 6: Schematic diagram of part of the NAD^+-binding domain in ALDH1 showing the two local structures, β7 (from residue G163 onward) and αD (from P171 onward). The bound NAD^+ and the other amino acid residues, E268, T244, and C302, are included to highlight their close proximity to β7 and αD in the ALDH1 structure.

the nonplanar reduced form of the nicotinamide ring would be tightly constrained by the positions of residues T244, E268, and the acyl group attached to C302 (*11*). The relaxation of these constraints might favor the binding of the extended conformation of coenzyme, which sterically occludes the deacylation step.

A role for T244 in coenzyme binding was evident from an inspection of the structural model of ALDH1. As shown in Figure 4, T244 lies close to E268, the essential general base needed to activate both C302 and water. On the basis of this model, it appears that the CG2 atom of T 244 is within van der Waals contact with the CB of E268. This contact will be lost in the mutant, potentially imparting additional conformational freedom to the side chain of E268. Excessive movement of the side chain would prevent the carboxylic group from occupying the proper conformation for the deacylation step and thereby result in the observed decrease in specific activity for the mutant. T244 is also close to a number of the amino acid residues that interact with NAD^+. The hydroxyl side chain of T244 forms a hydrogen bond with the amino group side chain of K178 (Figure 6). K178 is located on an α-helix, which forms part of the NAD^+ binding domain (*3*). Of equal importance are the van der Waals interactions between the CG2 atom of T244 and the CE and CG atoms of M174 and P167, respectively. P167 lies at the end of a β-strand and is positioned, along with residues 244 and 174, within 4 Å of the nicotinamide portion of the coenzyme. From the structure, it appears that the close packing contacts contributed by atoms from T244, P167, and M174 help maintain the spatial positions of the surrounding protein structure. Changes to these interactions could alter the nature of the contacts between the nicotinamide ring and the local structure of the active site. This could provide a structural explanation for why coenzyme binding is affected

in the T244S mutant as indicated by the decrease in the k_1 term (30-fold) and the increase in the K_{ia} value (9-fold). T244 is likely to have a direct role in binding the coenzyme in a productive conformation for hydride transfer because the methyl group could come within 2.7 Å of the extended nicotinamide ring (Figure 5). The additional methyl group of T244 could provide a more nonpolar character to this area of the active site and narrow the binding pocket for the nicotinamide ring. Understanding the effects of such small differences on coenzyme binding and the stability of the local structures will require a high-resolution X-ray crystallographic analysis of the enzyme binary complex with the coenzyme.

Though the important location of T244 has been recognized for some time (*3*, *4*, *9*), no site-specific alteration of this residue has been reported prior to our study. The novel insight in our study is that T244 can directly impact the deacylation step in which Mg^{2+} ions provide a 2-fold rate enhancement. This finding, together with an earlier observation (*5*) that E399 was important to hydride transfer, reveals that both T244 and E399 contribute stable binding interactions to the coenzyme, though each is related to a different step in ALDH catalysis. It is interesting that ALDH2 contains a threonine at the position corresponding to 244 in ALDH1, and yet, deacylation is rate-limiting for this isozyme. This implies that residue 244 alone does not impart this behavior; it is the combined contribution of T244 and its interactions with neighboring residues and the dynamic motion of the enzyme that determines the kinetics associated with the binding site for the nicotinamide ring. Hence, the dynamic aspects of their interactions could influence the residency times between the extended and the contracted conformations of the nicotinamide ring. In ALDH2, NAD^+ is thought to have a preference for an extended conformation because the rate-limiting step is not hydride transfer (*11*). This presumed preference is consistent with other data obtained through NMR (*12*), fluorescence spectroscopy (*12*), and X-ray crystallography (*11*). A comparison of the derived crystallographic coordinates from the ALDH1 and ALDH2 structures (*3*, *9*) indicates that the relative motion of the side chain of M174, as assessed by a comparison of Debye−Waller factors, in ALDH1 is greater than that in ALDH2. Thus, it is possible that the interaction between M174 and T244 in ALDH2 is more stable than that in ALDH1. This could in turn provide a more stable interaction between T244 and an extended nicotinamide conformation, resulting in an increase of the residency time for the latter conformation.

In this study, we showed how it was possible to select for an altered enzyme with a new rate-limiting step using a random mutation approach. Though our goal is to produce an enzyme with higher specific activity, finding a point mutation shows that it could be possible to select for ALDHs that possess more interesting properties.

REFERENCES

1. Perozich, J., Nicholas, H., Wang, B. C., Lindahl, R., and Hempel, J. (1999) Relationships within the aldehyde dehydrogenase extended family, *Protein Sci. 8*, 137−146.
2. Ehrig, T., Bosron, W. F., and Li, T. K. (1990) Alcohol and aldehyde dehydrogenase, *Alcohol Alcohol. (Oxford) 25*, 105−116.
3. Moore, S. A., Baker, H. M., Blythe, T. J., Kitson, K. E., Kitson, T. M., and Baker, E. N. (1998) Sheep liver cytosolic aldehyde dehydrogenase: the structure reveals the basis for the retinal specificity of class 1 aldehyde dehydrogenases, *Structure 6*, 1541−1551.
4. Steinmetz, C. G., Xie, P., Weiner, H., and Hurley, T. D. (1997) Structure of mitochondrial aldehyde dehydrogenase: the genetic component of ethanol aversion, *Structure 5*, 701−711.
5. Ho, K. K., Allali-Hassani, A., Hurley, T. D., and Weiner, H. (2005) Differential effects of Mg^{2+} ions on the individual kinetic steps of human cytosolic and mitochondrial aldehyde dehydrogenases, *Biochemistry 44*, 8022−8029.
6. Blackwell, L. F., Motion, R. L., MacGibbon, A. K., Hardman, M. J., and Buckley, P. D. (1987) Evidence that the slow conformation change controlling NADH release from the enzyme is rate-limiting during the oxidation of propionaldehyde by aldehyde dehydrogenase, *Biochem. J. 242*, 803−808.
7. Weiner, H., Hu, J. H., and Sanny, C. G. (1976) Rate-limiting steps for the esterase and dehydrogenase reaction catalyzed by horse liver aldehyde dehydrogenase, *J. Biol. Chem. 251*, 3853−3855.
8. Feldman, R. I., and Weiner, H. (1972) Horse liver aldehyde dehydrogenase. II. Kinetics and mechanistic implications of the dehydrogenase and esterase activity, *J. Biol. Chem. 247*, 267−272.
9. Ni, L., Zhou, J., Hurley, T. D., and Weiner, H. (1999) Human liver mitochondrial aldehyde dehydrogenase: three-dimensional structure and the restoration of solubility and activity of chimeric forms, *Protein Sci. 8*, 2784−2790.
10. Hurley, T. D., Perez-Miller, S., and Breen, H. (2001) Order and disorder in mitochondrial aldehyde dehydrogenase, *Chem.-Biol. Interact. 130*−*132*, 3−14.
11. Perez-Miller, S. J., and Hurley, T. D. (2003) Coenzyme isomerization is integral to catalysis in aldehyde dehydrogenase, *Biochemistry 42*, 7100−7109.
12. Hammen, P. K., Allali-Hassani, A., Hallenga, A., K., Hurley, T. D., and Weiner, H. (2002) Multiple conformations of NAD^+ and NADH when bound to human cytosolic and mitochondrial aldehyde dehydrogenase, *Biochemistry 41*, 7156−7168.
13. Ni, L., Sheikh, S., and Weiner, H. (1997) Involvement of glutamate 399 and lysine 192 in the mechanism of human liver mitochondrial aldehyde dehydrogenase, *J. Biol. Chem. 272*, 18823−18826.
14. Wang, X., and Weiner, H. (1995) Involvement of glutamate 268 in the active site of human liver mitochondrial (Class 2) aldehyde dehydrogenase as probed by site-directed mutagenesis, *Biochemistry 34*, 237−243.
15. Sheikh, S., Ni, L., Hurley, T. D., and Weiner, H. (1997) The potential roles of the conserved amino acids in human liver mitochondrial aldehyde dehydrogenase, *J. Biol. Chem. 272*, 18817−18822.
16. Tabor, S., and Richardson, C. C. (1985) A bacteriophage T7 RNA polymerase/promoter system for controlled exclusive expression of specific genes, *Proc. Natl. Acad. Sci. U.S.A. 82*, 1074−1078.
17. Zheng, C. F., Wang, T. T., and Weiner, H. (1993) Cloning and expression of the full-length cDNAs encoding human liver class 1 and class 2 aldehyde dehydrogenase, *Alcohol.: Clin. Exp. Res. 17*, 828−831.
18. Ghenbot, G., and Weiner, H. (1992) Purification of liver aldehyde dehydrogenase by *p*-hydroxyacetophenone-sepharose affinity matrix and the coelution of chloramphenicol acetyl transferase from the same matrix with recombinantly expressed aldehyde dehydrogenase, *Protein Expression Purif. 3*, 470−478.
19. Laemmli, U. K. (1970) Cleavage of structural proteins during the assembly of the head of bacteriophage T4, *Nature 227*, 680−685.
20. Plowman, K. M. (1972) *Enzyme Kinetics*, McGraw-Hill, New York.
21. Farres, J., Wang, X., Takahashi, K., Cunningham, S. J., Wang, T. T., and Weiner, H. (1994) Effects of changing glutamate 487 to lysine in rat and human liver mitochondrial aldehyde dehydrogenase. A model to study human (Oriental type) class 2 aldehyde dehydrogenase, *J. Biol. Chem. 269*, 13854−13860.
22. Vallari, R. C., and Pietruszko, R. (1984) Interaction of Mg^{2+} with human liver aldehyde dehydrogenase. II. Mechanism and site of interaction, *J. Biol. Chem. 259*, 4927−4933.
23. Plapp, B. V., (1995) Site-directed mutagenesis: A tool for studying enzyme catalysis, in *Enzyme Kinetics and Mechanism, Part D* (Purich, D. L., Ed.) Vol. 249, pp 91−119, Academic Press, New York.
24. Sidhu, R. S., and Blair, A. H. (1975) Human liver aldehdye dehydrogenase. Esterase activity, *J. Biol. Chem. 250*, 7894−7898.

25. Mukerjee, N., and Pietruszko, R. (1992) Human mitochondrial aldehyde dehydrogenase substrate specificity: Comparison of esterase with dehydrogenase reaction, *Arch. Biochem. Biophys. 299*, 23−29.
26. Kitson, T. M. (1989) Kinetics of *p*-nitrophenyl pivalate hydrolysis catalysed by cytoplasmic aldehyde dehydrogenase, *Biochem. J. 257*, 573−578.
27. Schwede, T., Kopp, J., Guex, N., and Peitsch, M. C. (2003) SWISS-MODEL: an automated protein-homology server, *Nucleic Acids Res. 31*, 3381−3385.
28. Guex, N., and Peitsch, M. C. (1997) SWISS-MODEL and Swiss-PdbViewer: An environment for comparative protein modeling, *Electrophoresis 18*, 2714−2723.
29. Peitsch, M. C. (1995) Protein modeling by E-mail, *Bio/Technology 13*, 658−660.
30. Farres, J., Wang, T. T. Y., Cunningham, S. J., and Weiner, H. (1995) Investigation of the active site cysteine residue of rat liver mitochondrial aldehyde dehydrogenase by site-directed mutagenesis, *Biochemistry 34*, 2592−2598.
31. Takahashi, K., and Weiner, H. (1980) Magnesium stimulation of catalytic activity of horse liver aldehyde dehydrogenase. Changes in molecular weight and catalytic sites, *J. Biol. Chem. 255*, 8206−8209.
32. Vallari, R. C., and Pietruszko, R. (1984) Interaction of Mg2+ with human liver aldehyde dehydrogenase. I. Species difference in the mitochondrial isozyme, *J. Biol. Chem. 259*, 4922−4926.
33. Dickinson, F. M., and Hart, G. J. (1982) Effects of Mg^{2+}, Ca^{2+} and Mn^{2+} on sheep liver cytoplasmic aldehyde dehydrogenase, *Biochem. J. 205*, 443−448.
34. Bennett, A. F., Buckley, P. D., and Blackwell, L. F. (1983) Inhibition of the dehydrogenase activity of sheep liver cytoplasmic aldehyde dehydrogenase by magnesium ions, *Biochemistry 22*, 776−784.
35. Wang, S. L., Wu, C. W., Cheng, T. C., Yin, S. J. (1990) Isolation of high-K_m aldehyde dehydrogenase isoenzymes from human gastric mucosa, *Biochem. Int. 22*, 199−204.
36. Lindahl, R., and Evces, S. (1984) Rat liver aldehyde dehydrogenase. II. Isolation and characterization of four inducible isozymes, *J. Biol. Chem. 259*, 11991−11996.
37. Chen, Z., Zhang, J., and Stamler, J. S. (2002) Identification of the enzymatic mechanism of nitroglyerin bioactivation. *Proc. Natl. Acad. Sci, U.S.A. 99*, 8306−8311.
38. Murphy, T. C., Arntzen, R., and Picklo, M. J., Sr. (2005) Nitrate-based vasodilators inhibit multiple vascular aldehyde dehydrogenases, *Cardiovasc. Toxicol. 5*, 321−332.
39. Li, Y., Zhang, D., Jin, W, Shao, C., Yan, P., Xu, C., Sheng, H., Liu, Y., Yu, J., Xie, Y., Zhao, Y., Lu, D., Nebert, D. W., Harrison, D. C., Huang, W., and Jin, L. (2006) Mitochondrial aldehyde dehydrogenase-2 (ALDH2) Glu504Lys polymorphism contributes to the variation in efficacy of sublingual nitroglycerin, *J. Clin. Invest. 116* (2), 506−511.
40. Dickinson, F. M., and Haywood, G. W. (1986) The effects of Mg^{2+} on certain steps in the mechanisms of the dehydrogenase and esterase reactions catalysed by sheep liver aldehyde dehydrogenase. Support for the view that dehydrogenase and esterase activities occur at the same site on the enzyme, *Biochem. J. 233*, 877−883.
41. Dalziel, K. (1957) Initial steady-state velocities in the evaluation of enzyme-coenzyme substrate reaction mechanisms, *Acta Chem. Scand. 11*, 1706−1723.

BI060718C